Published online 10 January 2015 *Nucleic Acids Research, 2015, Vol. 43, No. 3* ***1469–1484***
doi: 10.1093/nar/gku1382

Two novel NAC transcription factors regulate gene expression and flowering time by associating with the histone demethylase JMJ14

Yong-Qiang Ning[1], Ze-Yang Ma[1], Huan-Wei Huang[1], Huixian Mo[2], Ting-ting Zhao[1], Lin Li[1], Tao Cai[1], She Chen[1], Ligeng Ma[2] and Xin-Jian He[1,*]

[1]National Institute of Biological Sciences, Beijing 102206, China and [2]College of Life Sciences, Capital Normal University, Beijing 100048, China

Received June 13, 2014; Revised December 17, 2014; Accepted December 22, 2014

ABSTRACT

The histone demethylase JMJ14 catalyzes histone demethylation at lysine 4 of histone 3 and is involved in transcriptional repression and flowering time control in *Arabidopsis*. Here, we report that JMJ14 is physically associated with two previously uncharacterized NAC transcription factors, NAC050 and NAC052. The *NAC050/052-RNAi* plants and the CRISPR-CAS9-mediated *nac050/052* double mutant plants show an early flowering phenotype, which is similar to the phenotype of *jmj14*, suggesting a functional association between JMJ14 and NAC050/052. RNA-seq data indicated that hundreds of common target genes are co-regulated by JMJ14 and NAC50/052. Our ChIP analysis demonstrated that JMJ14 and NAC050 directly bind to co-upregulated genes shared in *jmj14* and *NAC050/052-RNAi*, thereby facilitating H3K4 demethylation and transcriptional repression. The NAC050/052 recognition DNA cis-element was identified by an electrophoretic mobility shift assay at the promoters of its target genes. Together, our study identifies two novel NAC transcription repressors and demonstrates that they are involved in transcriptional repression and flowering time control by associating with the histone demethylase JMJ14.

INTRODUCTION

Histone methylation affects transcription status on chromatin and is dynamically regulated through the addition and removal of methyl groups. The enzymes that contain an evolutionarily conserved SET domain (named after the three *Drosophila* histone methyltransferases Su(var)3–9, E(z) and Trithorax) catalyze histone lysine methylation (1,2). The JmjC domain-containing histone demethylases are responsible for the removal of methyl groups from methylated histone at lysine sites and are conserved in plants, animals and fungi (3,4).

In *Arabidopsis*, there are 21 JmjC domain-containing histone demethylases that have been named JMJ11–JMJ31 (5). Previous studies have demonstrated that the *Arabidopsis* JmjC domain-containing histone demethylases are involved in diverse biological processes (6). JMJ25/IBM1 (Increase in Bonsai Methylation 1), which is necessary for floral development, is responsible for H3K9 demethylation at actively transcribed genes and protects these genes from DNA methylation at CHG sites (7–9). JMJ30/JMJD5 positively affects circadian clock-regulated gene expression and is involved in controlling the circadian rhythm (10,11). The histone arginine demethylases JMJ20 and JMJ22 act as positive regulators of seed germination by mediating the removal of repressive histone arginine methylation and the transcriptional activation at *GA3ox1* and *GA3ox2* (12). ELF6/JMJ11 and REF6/JMJ12 are two close homologs that control flowering time and other developmental processes (11,13,14). REF6 acts as an H3K27me3 demethylase and contributes to the expression of genes involved in development and stress response (11). Although these JmjC histone demethylases were identified and characterized in *Arabidopsis*, further studies are required to clarify how conserved histone demethylases have different target genes and are involved in diverse biological processes.

The H3K4 demethylase JMJ14 is involved in repression of the floral integrator genes *FT* and *SOC1* (15–17). Moreover, JMJ14 is required for maintenance of transcriptional silencing through an RNA-directed DNA methylation pathway (15,18). Interestingly, JMJ14 is involved in transcriptional repression of aberrant RNAs, which trigger post-transcriptional gene silencing (19). The close homologs of JMJ14, JMJ15 and JMJ18, regulate flowering time through reducing H3K4 trimethylation at the floral repressor gene *FLC*, resulting in the repression of *FLC* expression and the promotion of flowering time (20,21). The role

*To whom correspondence should be addressed. Tel: +86 10 80707712; Fax: +86 10 80707715; Email: hexinjian@nibs.ac.cn

of JMJ15 and JMJ18 in flowering promotion is opposite to that of JMJ14 in flowering repression.

The mammalian histone demethylases usually interact with transcriptional regulators to control gene expression for specific target genes. The JmjC histone demethylase JHDM2A/JMJD1a interacts with the androgen receptor and cause the removal of H3K9 demethylation, resulting in the transcriptional activation of androgen receptor target genes (22). JARID1C/SMCX and the transcription repressor REST interact with each other and occupy the promoters of REST target genes (23). The depletion of JARID1C increases H3K4 trimethylation and simultaneously induces the expression of REST target genes that are implicated in X-linked mental retardation and epilepsy. JARID1a forms a complex with the CLOCK-BMAL1 transcription factors, influencing the circadian clock by activating the transcription of Per2 (24).

The plant-specific NAC (NAM, ATAF1 and CUC1/CUC2) proteins form one of the largest transcription factor families in plants (25–27). NAC transcription factors are involved in various biological processes, including development, hormone signaling, senescence and biotic and abiotic stress responses (26,27). NAC transcription factors contain a conserved N-terminal DNA-binding NAC domain and a diversified C-terminal transcription regulatory domain. Previous studies have demonstrated that many NAC proteins are transcriptional activators, whereas a few others are transcription repressors (26–29). NAC proteins are recruited to their target loci by directly binding the DNA-cis element in the promoter of their target genes (26,27).

JMJ14 is involved in transcriptional gene silencing and flowering time regulation (15–18), but we do not know how JMJ14 specifically functions at a subset of genes but not others. Given that several histone demethylases exist in protein complexes in animals (22–24,30), we asked whether JMJ14 associates with any other proteins in *Arabidopsis*. Thus, we generated *JMJ14–3xFlag* transgenic plants to affinity purify JMJ14-associated proteins and identify these proteins by mass spectrometry. Our study demonstrates that JMJ14 and two previously uncharacterized NAC transcription factors, NAC050 and NAC052, associate with each other and co-occupy hundreds of common target genes, resulting in H3K4 demethylation and transcriptional repression.

MATERIALS AND METHODS

Plant materials, constructs and growth conditions

The *Arabidopsis* materials included the wild-type (WT) Col-0, *jmj14* (Salk_135712C) and *NAC050/52-RNAi* plants. Two inverted copies of the *NAC050* cDNA fragment (+489∼+1077) were separately inserted into the RNAi vector *pFGC5941* and transformed into the WT and *jmj14* plants for the knockdown of *NAC050* and *NAC052* in *Arabidopsis*. This fragment of the *NAC050* cDNA sequence is highly similar to *NAC052*, but is different from any other genes. Thus, both *NAC050* and *NAC052* were knocked down in the *NAC050/52-RNAi* plants. We generated the native promoter-driven *JMJ14–3xFlag*, *NAC050–3xMyc* and *NAC052–3xMyc* constructs in the modified *pCAMBIA1305* backbone. The length of the promoters for *JMJ14*, *NAC050* and *NAC052* is 1538, 1438 and 1772 bp, respectively. The sequences of the primers used in amplification of *JMJ14*, *NAC050* and *NAC052* are shown in Supplementary Table S1. *JMJ14–3xFlag* was ligated with the KpnI and PstI sites, whereas either *NAC050–3xMyc* or *NAC052–3xMyc* was ligated with the PstI and BamHI sites. The *JMJ14–3xFlag* construct was transformed into the WT, *jmj14* and *NAC050/052-RNAi* plants for the JMJ14 chromatin immunoprecipitation (ChIP) assay, whereas the *NAC050×3xMyc* construct was transformed into the WT and *jmj14* plants for the NAC050 ChIP assay.

For co-immunoprecipitation (co-IP), either the *NAC050–3xMyc* or *NAC052–3xMyc* construct was introduced into the WT and *JMJ14–3xFlag* transgenic plants. The full-length *NAC050* cDNA was cloned downstream of the *35S* promoter sequence in the modified *pCAMBIA1300* vector. The *35S-NAC050* construct was transformed into the WT plants to generate *NAC050* overexpression lines. All of the constructs that were used in this study were transformed by *Agrobacterium* infection. The T1 seedlings were grown on Murashige and Skoog (MS) medium that was supplemented with antibiotics. The *Arabidopsis* seedlings that were used for the analyses of the molecular and developmental phenotypes were grown on MS medium under long-day conditions (16 h day and 8 h night) at 22°C. The seedlings were transplanted into soil and grown under the same conditions for the examination of the flowering time.

Affinity purification and mass spectrometric analysis

We collected flowers at stages 1–15 of floral development from 1-month-old plants for isolating protein extract. Protein extraction was performed according to the method previously described (31) and subjected to the affinity purification of JMJ14–3xFlag using an anti-Flag antibody. For the affinity purification, Anti-Flag M2 Affinity Gel (Sigma, A2220) was added to the protein extract and incubated in lysis buffer at 4°C for 2–4 h. The agarose-bound proteins were precipitated by centrifugation and washed four times, followed by an elution with the 3xFlag peptide (Sigma, F4799). The eluted proteins were run on a 10% sodium dodecyl sulphate-polyacrylamide gel electrophoresis (SDS-PAGE) gel and visualized by silver staining (Sigma, PROTSIL1). The proteins were extracted from the gel and analyzed by tandem mass spectrometry as previously described (31). A search was conducted to see if the obtained peptide sequence data could be found in the International Protein Index database of *Arabidopsis* on the Mascot server (Matrix Science Ltd., London, UK).

Co-IP and gel filtration

The *NAC050–3xMyc* and *NAC052–3xMyc* constructs were separately transformed into *JMJ14–3xFlag* transgenic plants. The offspring seedlings harboring both the *JMJ14–3xFlag* and *NAC050–3xMyc* or *NAC052–3xMyc* transgenes were used to determine whether JMJ14 interacts with NAC050 or NAC052 by co-IP. Anti-Flag M2 Affinity Gel (Sigma, A2220) was added to the protein extract and incubated at 4°C for 2–4 h. The agarose-bound proteins were

precipitated by centrifugation and washed four times. The precipitate was suspended, boiled in 1× SDS sample buffer and run on an SDS-PAGE gel for western blotting. The protein extracts from *JMJ14–3xFlag*, *NAC050–3xMyc* and *NAC052–3xMyc* transgenic plants were used for gel filtration. The protein extracts were loaded onto a Superose 6 10/300 GL column (GE Healthcare, 17–5172–01) and harvested once per 500 μl. The indicated fractions were run on a 10–12% SDS-PAGE gel and subjected to western blotting. Anti-Flag (Abmart, M20008L) and anti-Myc antibodies (Abmart, M20002L) were used in the western blotting for both the co-IP and gel filtration assays.

Yeast two-hybrid assay

The full-length cDNA sequences of *JMJ14*, *NAC050* and *NAC052* were separately cloned into the yeast vectors *pGADT7* and *pGBKT7* to examine the interactions between JMJ14, NAC050 and NAC052. The full-length cDNA of *JMJ14* (2865 bp) was amplified and cloned into the *pGADT7* vector between the XmaI and XhoI sites and into the *pGBKT7* vector between the XmaI and PstI sites. The full-length cDNAs of *NAC050* (1341 bp) and *NAC052* (1353 bp) were separately cloned into both the *pGADT7* and *pGBKT7* vectors between the EcoRI and BamHI sites. Truncated *JMJ14* and *NAC050* sequences were cloned into *pGADT7* or *pGBKT7* to determine the domains in JMJ14 and NAC050 that are required for the interaction.

For cloning the truncated *JMJ14* sequences into *pGADT7*, all the truncated *JMJ14* sequences were amplified from the above *pGADT7-JMJ14* plasmid. The *JMJ14-a/b/c* fragments were amplified using the primers *JMJ14ADBD-Xma I* and *JMJ14AD-a/b/c-R*, whereas the *JMJ14-e/d/f* fragments were amplified using the primers *JMJ14AD-d/e/f-F* and *JMJ14AD-Xho I*. These fragments were digested with corresponding restriction enzymes and cloned into the *pGADT7* vector. For cloning the truncated *NAC050* sequences into *pGBKT7*, all the truncated *NAC050* sequences were amplified from the *pGBKT7-NAC050* plasmid. *NAC050-a/c* were amplified using the primers *NAC050ADBD-EcoR I* and *NAC050BD-a/c-R*, whereas *NAC050-BD-b/d* were amplified using the primers *NAC050BD-b/d-F* and *NAC050ADBD-BamH I*. The primers that were used for cloning the full-length and truncated sequences are listed in Supplementary Table S1. Different combinations of the *pGADT7* and *pGBKT7* constructs were transformed into the yeast strain Y1348. The positive strains were selected from a synthetic dropout medium minus Trp and Leu (SD-TL) and then used for a growth assay on SD-TLH (the synthetic dropout medium minus Trp, Leu and His) supplemented with 20 mM 3-AT. These strains were simultaneously grown on SD-TL as controls.

RNA deep sequencing and data analysis

The WT Col-0, *jmj14* and *NAC050/052-RNAi* were grown on MS medium under long-day conditions (16 h day and 8 h night) at 22°C. Total RNA was extracted from 2-week-old seedlings followed by the construction of mRNA libraries. The mRNA libraries were sent to BGI (Shenzhen, China) for single-end Illumina sequencing. After the adaptor sequences were removed, 45-bp reads were mapped to the *Arabidopsis* genome that was downloaded from TAIR10 (http://www.arabidopsis.org/) using the TopHat v2.0.6 program (32). RNA reads that were uniquely mapped to the genome with a maximum of two mismatches were included in the gene expression analysis. Gene expression differences were evaluated using a combination of Fisher's exact test ($P < 0.01$) and the fold change of the normalized reads (Log2(fold change) > 0.5). The Gplots package in R was used to draw a heat map of the differentially expressed genes.

Analyses of RNA transcripts by reverse transcriptase-PCR (RT-PCR)

Total RNA was isolated from 2-week-old seedlings that were grown on MS medium plates as previously described (31). The RNA was treated with DNase to remove DNA contamination and subjected to quantitative RT-PCR using a one-step RT-PCR kit (Takara, RR018A). Oligo-dT was used as the primer for reverse transcription. The expression of *ACT2* was examined as an internal control. The expression of each gene that was tested in this study was normalized to the expression of *ACT2*. 'No RT' indicates that the RNA samples were directly used as templates to amplify the control gene. The primers that were used for the PCR are listed in Supplementary Table S1.

Electrophoretic mobility shift assay (EMSA)

The full-length *NAC050/052* cDNA sequences were cloned in frame with the 5′-terminal GST sequence in the *pGEX-4T-1* vector. Meanwhile, the *NAC050* cDNA sequences of the N-terminal NAC domain (1–678 bp) and the C-terminal regulatory domain (679–1341 bp) were cloned into the *pGEX-4T-1* vector and the corresponding truncated NAC050 proteins were defined as NAC050-N and NAC050-C, respectively.

The GST-fusion proteins were expressed in the *E. coli* strain BL21 (Invitrogen), purified with Glutathione Sepharose 4B (GE Healthcare,17075601) and used for EMSA. One microgram of purified protein was incubated with 0.08 nM of each double-stranded DNA oligo in a binding buffer at 25°C for 30 min. The binding buffer contained 25 mM HEPES (pH 7.6), 50 mM KCl, 0.1 mM ethylenediaminetetraacetic acid (pH 8.0), 12.5 mM $MgCl_2$, 1 mM DTT, 0.5% (w/v) bovine serum albumin and 5% (w/v) glycerol. The binding reaction mixture was loaded onto a 7% non-denaturing polyacrylamide gel at 80 V for 2 h, and the bound DNAs were visualized by ethidium bromide staining.

ChIP assay

The association of JMJ14, NAC050 and H3K4me3 with chromatin was determined using a ChIP assay. Two-week-old seedlings were subjected to cross-linking in 0.5% formaldehyde under vacuum conditions. Thereafter, the nuclei were extracted from the seedlings and sonicated for chromatin extraction. Anti-Flag M2 Affinity Gel (Sigma,

A2220) and Anti-Myc Affinity Gel (Sigma, A7470) were used for the IP of JMJ14–3xFlag and NAC050–3xMyc, respectively. For H3K4me3 ChIP, anti-H3K4me3 antibody (Millipore, 05–745) were conjugated with Protein A agarose (Millipore, 16–157) followed by IP. The precipitate was analyzed by quantitative PCR. The ChIP-PCR experiments were biologically repeated and the same results were obtained. Showing is the results of three technical replicates from a representative experiment. The association of these proteins with the actin gene *ACT2* was examined and used as an internal control. The primers that were used for the PCR are listed in Supplementary Table S1. H3K4me3 ChIP-seq analysis was performed as previously described (33,34).

ChIP-seq data analysis

For H3K4me3 ChIP-seq data analysis, reads were mapped to the *Arabidopsis* genome (TAIR10, http://www.arabidopsis.org) with Bowtie (v0.12.7) with at most two mismatches (35). The package MACS (v1.4.2) was used to identify regions of H3K4me3 enrichment in *jmj14* and *NAC050/052-RNAi* as compared to the WT (36). Only peaks with *P*-value <0.001 and fold-change >2 were identified as differentially enriched regions. To determine the relationship between H3K4m3 enrichment and differentially expressed genes, we used R to plot the H3K4me3 pattern for differentially expressed genes. Each gene was divided into 50 intervals (2% for each interval), and the 1-kb regions upstream and downstream of each gene were divided into 20-bp intervals. Normalized reads in each interval was graphed to indicate the distribution of H3K4me3 across genes.

CRISPR-CAS9-mediated mutation

The DNA sequences of *NAC050* and *NAC052* are highly similar to each other. To produce a gRNA that directs their common target sequence GAAGGTTAATGATCTCCAGA, we synthesized two DNA oligos: *NAC050/052* oligo1 and *NAC050/052* oligo2 (Supplementary Table S1), which were annealed to form a double-stranded DNA and then inserted into the cloning vector harboring the *psgRNA-CAS9-At* fragment (37). Thereafter, the whole *psgRNA-CAS9-At* fragment was digested by EcoRI and HindIII and inserted into the corresponding sites of *pCambia1300* for agrobacterium-mediated transformation in *Arabidopsis*. The T1 transgenic plants were grown on MS medium supplemented with 30 mg/l hygromycin, and the resistant positive seedlings were selected for sequencing the target sequences of *NAC050* and *NAC052*. The homozygous mutants were acquired from T3 transgenic plants.

Transient luciferase reporter assay

A luciferase gene was driven by the promoter sequences of *AT2G18720* (−562 ∼ −52 bp), *AT2G21640* (−884 ∼ −470 bp), *AT5G16020* (−488 ∼ −1 bp) and *AT1G02580* (−500 ∼ −22 bp) at the KpnI-BamHI site of the modified *pCAMBIA1300* vector. Moreover, we generated a construct, in which the luciferase reporter gene was driven by a minimal *35S* promoter with an upstream GAL4-binding site. The reporter can be activated by the GAL4-DBD-VP16 fusion protein. The 5xNAC050-binding motif (CTTGGTCGCCACGGAA) as well as its mutant variant (CTTGGTCGCCCCGGAA) were separately ligated with 3′-end of the *35S* minimal promoter in the regulator construct to determine the function of the NAC050-binding motif. The luciferase reporter assay was performed in *Arabidopsis* mesophyll protoplasts as described by Sheen's group (http://genetics.mgh.harvard.edu/sheenweb/protocols_reg.html) with minor modifications. The luciferase activity was measured with Dual-Luciferase® Reporter Assay System (Promega, E1910). Three technical replicates from a representative experiment were shown.

RESULTS

JMJ14 is physically associated with the NAC transcription factors NAC050 and NAC052

To study how JMJ14 functions *in vivo*, we generated a construct harboring a native promoter-driven *JMJ14* genomic sequence with its C-terminus in frame with the *3xFlag* epitope tag and transformed the cassette into *Arabidopsis*. The expression of the *JMJ14–3xFlag* transgene in transgenic plants was determined by a western blotting assay (Supplementary Figures S1 and S2). We demonstrated that the *JMJ14–3xFlag* transgene complements the early flowering phenotype of the *jmj14* mutant (Supplementary Figure S1), suggesting that the *JMJ14–3xFlag* transgene functions as well as the corresponding endogenous gene. Based on previous transcriptome data (Supplementary Table S2), *NAC050/052* and *JMJ14* are highly expressed in floral organs and moderately expressed in other organs. Thus, flowers were collected from 1-month-old plants and used for affinity purification of JMJ14–3xFlag by anti-Flag antibody-conjugated agarose. Purified proteins were subjected to a mass spectrometric assay. Two previously uncharacterized NAC transcription factors, NAC050 (AT3G10480) and NAC052 (AT3G10490), were identified in co-purified proteins (Figure 1A). The two *NAC* genes form tandem repeats on the genome and may originate from a recent duplication. The N-terminal NAC domains of NAC050 and NAC052 are highly conserved in the NAC family proteins, while their C-terminal regions are similar to each other but are distinct compared to those of other NAC family proteins (Supplementary Figure S3).

To confirm the association between JMJ14 and the two NAC proteins, we introduced the native promoter-driven *NAC050–3xMyc* and *NAC052–3xMyc* transgenes into the *JMJ14–3xFlag* transgenic plants. The offspring plants harboring both *JMJ14–3xFlag* and *NAC050–3xMyc* or *NAC052–3xMyc* were used for co-IP. The protein extracts were precipitated by anti-Flag antibody followed by western blotting assay. The results indicate that JMJ14 can interact with both NAC050 and NAC052 (Figure 1B). To clarify whether the possible DNA binding ability of JMJ14 or NAC050/052 is required for the interaction between JMJ14 and NAC050/052, we performed co-IP after the protein extracts were treated with DNase (Supplementary Figure S2) and found that the addition of DNase has no effect

A

Accession number	Protein description	Mascot score	MW (Da)	Matched queries	Matched peptides
IPI00516310	JMJ14	30551	108087	837	65
IPI00536055	NAC050	515	50196	20	5
IPI00543522	NAC052	467	51260	19	5

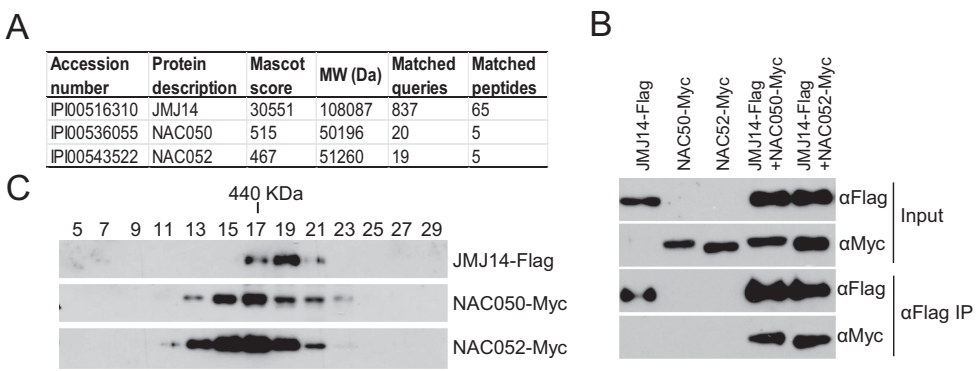

Figure 1. JMJ14 associates with NAC050 and NAC052 *in vivo*. (A) The NAC transcription factors NAC050 and NAC052 were identified in proteins that were co-purified with JMJ14 in a mass spectrometric assay. The protein extract was isolated from flowers of 1-month-old plants. (B) The interaction of JMJ14 with NAC050 and NAC052 was determined by co-IP. The *JMJ14–3xFlag* transgenic plants were crossed with *NAC050–3xMyc* and *NAC052–3xMyc* transgenic plants. The offspring harboring both of the epitope tags was used in the co-IP analysis. The parent *JMJ14–3xFlag*, *NAC050–3xMyc* and *NAC052–3xMyc* transgenic plants were used as controls. Two-week-old seedlings were used for protein extract. (C) Gel filtration assay of the protein extracts from *JMJ14–3xFlag*, *NAC050–3xMyc* and *NAC052–3xMyc* transgenic plants. The protein extract was isolated from flowers of 1-month-old plants.

on the interaction between JMJ14 and NAC050/052, indicating that the interaction is independent of the binding of JMJ14 and NAC050/052 to chromatin. By gel filtration, we found that NAC050 and NAC052 were co-eluted at the fractions between 13 and 21 (Figure 1C), suggesting that the two NAC proteins may form a tight complex *in vivo*. The result are consistent the yeast two-hybrid data indicating that NAC050 and NAC052 interact with each other (Figure 2A). JMJ14 was eluted at the fractions between 17 and 21, in which NAC050 and NAC052 were also eluted (Figure 1C). The results suggest that the JMJ14-NAC050/052 complex exists in the fractions between 17 and 21. However, although JMJ14 has a peak at the fraction of 19, NAC050 and NAC052 have a peak at the fraction of 17 but not 19 (Figure 1C). Thus, the JMJ14-NAC050/052 complex is not the only form of NAC050/052 *in vivo*. Some other uncharacterized proteins may associate with NAC050/052 and form an additional ∼440-KDa complex.

The FYRC domain of JMJ14 is responsible for binding NAC050 and NAC052

We performed a yeast two-hybrid assay to examine the interaction between JMJ14 and the two NAC proteins, demonstrating that JMJ14 not only interacts with NAC050 but also with NAC052 (Figure 2A). We also determined whether JMJ15 and JMJ18, two close homologs of JMJ14 (Supplementary Figure S4), interact with NAC050 and NAC052 by yeast two-hybrid. The results indicate that JMJ15 and JMJ18 fail to interact with the two NAC proteins (Supplementary Figure S5), suggesting the functional specificity of JMJ14 in the association with NAC050 and NAC052.

Our gel filtration assay indicated that NAC050 and NAC052 form ∼440-KDa complexes, which are much greater than the sizes of their monomers (Figure 1C). Thus, we performed a yeast two-hybrid assay to test whether the two NAC transcription factors interact with each other. The results indicate that NAC050 interacts not only with NAC050 but also with NAC052, whereas NAC052 cannot interact with NAC052 (Figure 2A). Based on the approximate size of the NAC050/052 complex, we propose that NAC050 and NAC052 may form tetramers or even higher molecular weight oligomers in *Arabidopsis*.

To determine the domain of JMJ14 that is required for association with the two NAC proteins, we cloned a series of truncated *JMJ14* sequences for the yeast two-hybrid assay (Figure 2B). The FYRC domain of JMJ14 by itself (JMJ14-f) is sufficient for the interaction of JMJ14 with NAC052 but not with NAC050 (Figure 2B and C). For the interaction of JMJ14 with NAC050, not only the FYRC domain but also the two other domains JmjC and C5HC2 are required (Figure 2B and C). The truncated JMJ14 sequences JMJ14-a and JMJ14-b without the FYRC domain cannot interact with NAC050 and NAC052 (Figure 2B and C). Therefore, the FYRC domain is necessary for the interaction of JMJ14 with both NAC050 and NAC052 as determined by the yeast two-hybrid assay. We further investigated whether the FYRC domain is required for the interaction of JMJ14 with NAC050 and NAC052 in *Arabidopsis*. A truncated *JMJ14* genomic sequence was constructed in frame with *3xFlag* and transformed into *NAC050–3xMyc* and *NAC052–3xMyc* transgenic plants (Figure 2D). The truncated *JMJ14* genomic sequence encodes a JMJ14 fragment that is equivalent to JMJ14-a used in the yeast two-hybrid assay (Figure 2B and C). The plants that express both *JMJ14-a-3xFlag* and *NAC050–3xMyc* or *NAC052–3xMyc* were used to determine the interaction of JMJ14-a with NAC050 and NAC052 by co-IP. The results indicate that NAC050–3xMyc and NAC052–3xMyc co-precipitate with JMJ14–3xFlag but not with JMJ14-a-3xFlag (Figure 2D), suggesting that the FYRC domain is required for the interaction of JMJ14 with NAC050 and NAC052 in *Arabidopsis*. To determine which domain in NAC050 is necessary for the interaction of NAC050 with JMJ14, we cloned a series of truncated *NAC050* sequences were cloned in the *pGAL4-BD* vector and used for the yeast two-hybrid assay (Supplementary Figure S6A). None of the truncated NAC050 sequences could interact with JMJ14 (Supplementary Figure S6B), suggesting that the full-length NAC050 is required for the interaction with JMJ14.

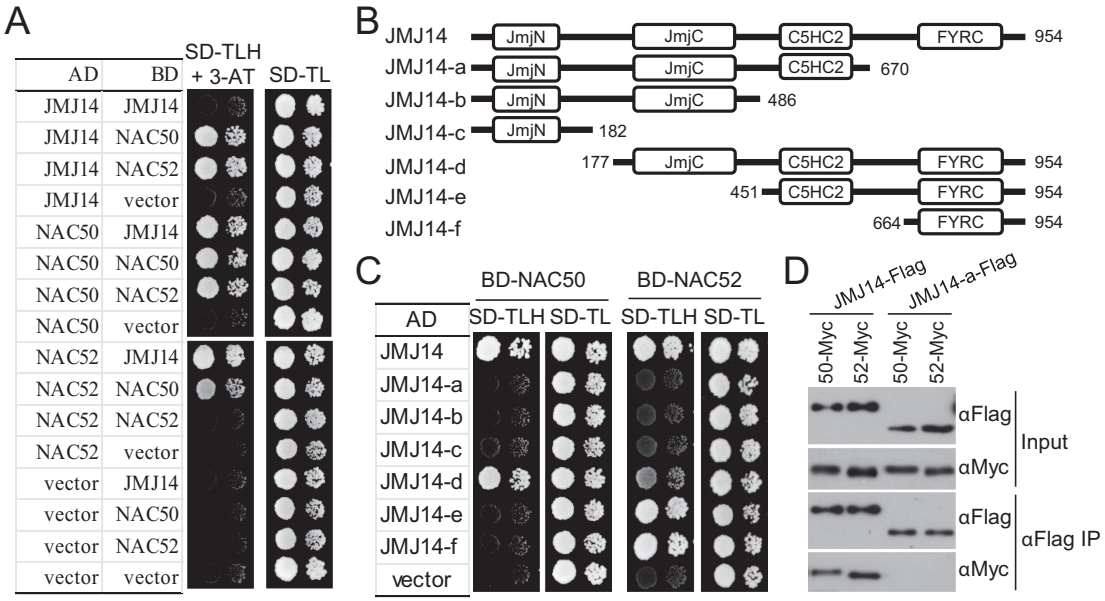

Figure 2. The FYRC domain is required for the interaction of JMJ14 with NAC050 and NAC052. (A) The interaction of JMJ14 with NAC050 and NAC052 was determined by the yeast two-hybrid assay. The full-length cDNA sequences of *JMJ14*, *NAC050* and *NAC052* were cloned into the yeast vectors *pGADT7* and *pGBKT7*. The constructs were transformed into the yeast strain Y1348 as indicated and then subjected to a growth assay on SD-TLH (synthetic dropout medium minus Trp, Leu and His) supplemented with 20 mM 3-AT as well as on SD-TL. (B) Diagram of the full-length and truncated versions of JMJ14. The conserved domains JmjN, JmjC, C5HC2 and FYRC are indicated. (C) Different JMJ14 cDNA fragments were cloned into *pGADT7*. The constructs harboring each of the JMJ14 sequences, as well as *pGBKT7-NAC050 or pGBKT7-NAC052*, were co-transformed into the yeast strain Y1348 for growth assays. (D) Either the full-length *JMJ14–3xFlag* or the truncated *JMJ14-a-3xFlag* transgene was introduced into *NAC-050–3xMyc* or *NAC052–3xMyc* transgenic plants. The transgenic plants were used to determine the interaction of the full-length and truncated JMJ14 with NAC050 or NAC052 by co-IP. The protein extract for co-IP was isolated from 2-week-old seedlings.

JMJ14 is functionally associated with NAC050 and NAC052 in flowering time regulation

Previous studies indicated that the *jmj14* mutant shows an early flowering phenotype, suggesting that JMJ14 is involved in the repression of flowering (13,15,16). We examined whether JMJ14 is functionally associated with NAC050 and NAC052 in flowering time regulation. No mutant of *NAC050* and *NAC052* is available in the *Arabidopsis* Biological Resource Center. To determine the biological function of the two NAC proteins, we generated an RNAi construct targeting *NAC050*. Because of the high sequence similarity between *NAC050* and *NAC052*, both of the *NAC* genes were reduced by the RNAi construct (Figure 3A). In the two individual *NAC050/052-RNAi* lines 8 and 11, the expression of *NAC050* and *NAC052* was effectively knocked down (Figure 3A). The *NAC050* cDNA fragment used for the *RNAi* construct was selected from the diversified region rather than from the conserved region of the *NAC* family genes to avoid affecting gene expression of other *NACs*. In the *jmj14* mutant, the expression of *NAC050* and *NAC052* is increased (Figure 3A). This feedback effect of *jmj14* indicates that NAC050 and NAC052 are functionally associated with JMJ14. The early flowering phenotype was not only found in *jmj14* but also in the two *NAC050/052-RNAi* lines. The numbers of rosette leaves upon flowering are comparable between *jmj14* and the two *NAC050/052-RNAi* lines but are significantly less than those in the WT (Figure 3B). We transformed the *35S-NAC050* construct into WT plants and determined the flowering time of the transgenic plants. RT-PCR indicated that *NAC050* was markedly overexpressed in two independent *35S-NAC050* transgenic plants (Figure 3C). As expected, the flowering time of the two *NAC050* overexpression lines was significantly delayed compared to that of the WT (Figure 3D). These results suggest that NAC050 and NAC052 are functionally associated with JMJ14 and contribute to repression of flowering.

The early flowering phenotype of *jmj14* was previously reported to be associated with increased expression of floral integrator genes (13,16). Quantitative RT-PCR indicated that the transcript levels of the floral integrator genes *FT*, *LFY* and *PI* were weakly increased by *jmj14* as well as by the two individual *NAC050/052-RNAi* lines (Figure 3E), suggesting that the early flowering phenotype caused by *jmj14* and *NAC050/052-RNAi* is correlated with the increased expression of these floral integrator genes. We further determined whether the overexpression of *NAC050* in the *35S-NAC050* transgenic plants represses the expression of *FT*, *LFY* and *PI*. The results show that the expression of *FT* and *PI* is reduced in the *NAC050* overexpression lines relative to that in the WT (Figure 3E), suggesting that NAC050 represses the expression of *FT* and *PI*. The delayed flowering time in the *NAC050* overexpression lines is correlated with the reduced expression of *FT*, *PI* and possibly other uncharacterized floral integrator genes. Different from *FT* and *PI*, the expression level of *LFY* is comparable between the WT and the *NAC050* overexpression lines (Figure 3E), suggesting that the WT expression level of *NAC050* is sufficient for properly repressing the expression of *LFY*.

Involvement of JMJ14 in flowering time control was previously reported by several independent groups, but the un-

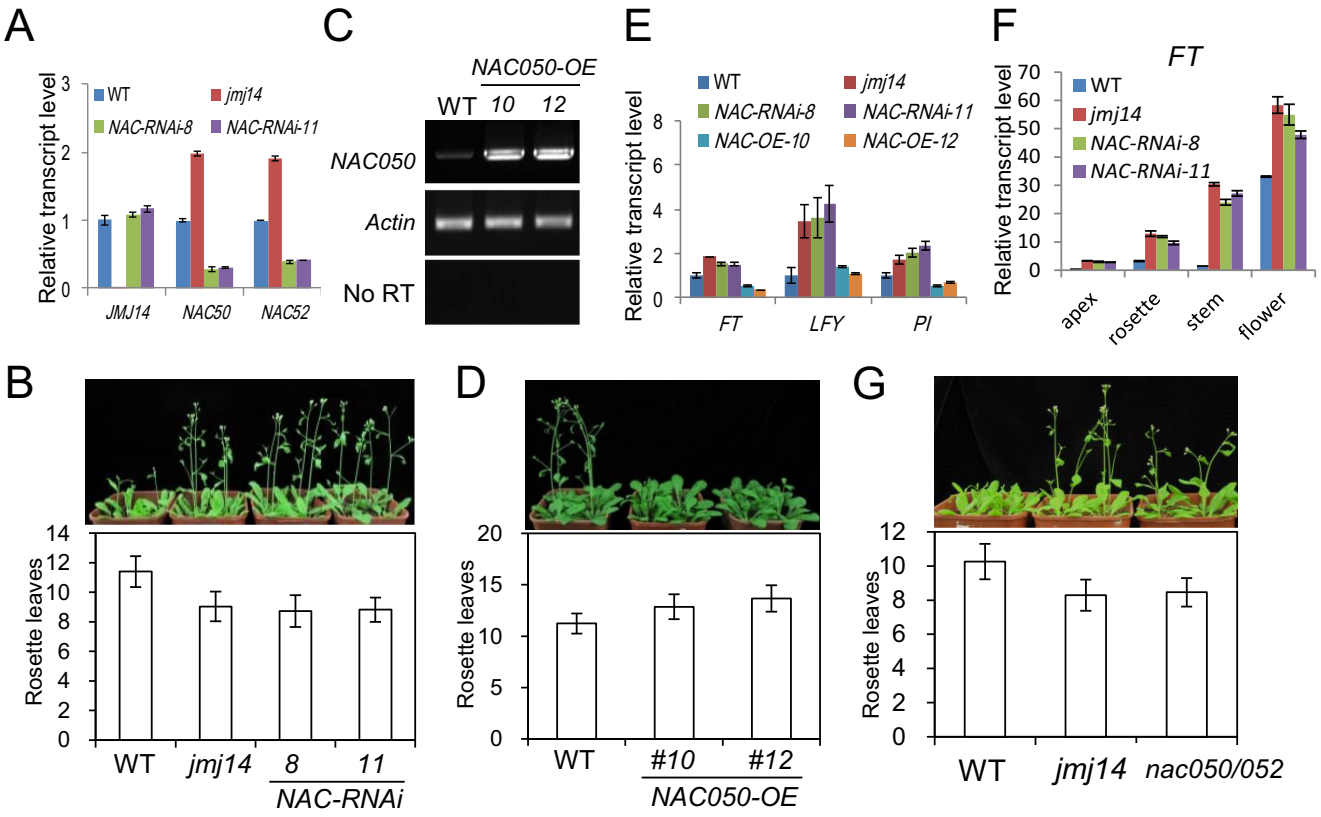

Figure 3. Functional association between JMJ14 and NAC050/052 in flowering time regulation. (A) Quantitative RT-PCR was performed to determine the transcript levels of *JMJ14*, *NAC050* and *NAC052* in the WT, *jmj14* and two independent *NAC050/052* knockdown lines, *NAC-RNAi-8* and *NAC-RNAi-11*. Total RNA used for RT-PCR was extracted from 2-week-old seedlings. The actin gene was used as an internal control. The results of three replicates are shown. (B) Shown are the WT, *jmj14*, *NAC-RNAi-8* and *NAC-RNAi-11* plants that were grown on soil under long-day conditions. The flowering time was assessed by counting rosette leaves. At least 20 plants of each genotype were used to count the rosette leaves. The average and standard deviation are indicated in the chart. (C) The transcript level of *NAC050* was determined by RT-PCR in the WT and two individual *35S-NAC050* transgenic lines *#10* and *#12*. The actin gene was used as a control. 'No RT' stands for amplification of the actin gene without reverse transcription. (D) The WT and *35S-NAC050* transgenic plants were grown on soil under long-day conditions. The numbers of rosette leaves from at least 20 plants were included to calculate the average and standard deviation. (E) The effect of *jmj14* and *NAC050/052-RNAi* on the expression of floral integrator genes. The expression of the floral integrator genes *FT*, *LFY* and *PI* in the WT, *jmj14* and two individual *NAC050/052-RNAi* lines was determined by quantitative RT-PCR. The experiment was biologically repeated and the results of three technical replicates from a representative experiment are shown. (F) The effect of *jmj14* and *NAC050/052-RNAi* on the expression of *FT* in different tissues of 1-month-old plants. The results of three replicates are shown. (G) The CRISPR-mediated *nac050/052* double mutant shows an early flowering phenotype. Soil-grown plants were photographed 3 weeks after planting.

derlying mechanism is controversial (13,15–17). Jeong *et al.* reported that JMJ14 directly targets the floral integrator gene *FT* and acts in histone H3K4 demethylation and transcriptional repression at the locus. However, another study indicated that the effect of *jmj14* on *FT* expression is unrelated to H3K4me3 (16), which argues against the direct role of JMJ14 in the repression of *FT*. We found that although the expression of *FT*, *LFY* and *PI* is increased in *jmj14*, H3K4me3 of the three genes is not significantly altered in *jmj14* (Supplementary Figure S7), suggesting that *FT*, *LFY* and *PI* are not the direct targets of JMJ14. Based on the online transcriptome data (38), we found that *JMJ14* and *NAC050/052* are co-expressed in different tissues during various developmental stages (Supplementary Tables S2 and Figure S8), supporting the notion that JMJ14 and NAC50/052 act together. We performed quantitative RT-PCR to determine whether *jmj14* and *NAC050/052-RNAi* affect the expression of *FT* in different tissues including shoot apex, rosette leaf, stem and flower. We found that the expression of *FT* is upregulated not only by *jmj14* but also by *NAC050/052-RNAi* in all the tissues tested in 1-month-old plants (Figure 3F), suggesting that JMJ14 and NAC050/52 affect the expression of *FT* in different tissues during various development stages. Furthermore, we obtained *jmj14 ft* and *jmj14 fve* double mutants by crossing *jmj14* with two late-flowering mutants *ft* and *fve*, respectively. The flowering time is markedly promoted in *jmj14 fve* compared to *fve*, confirming that JMJ14 is involved in flowering time regulation (Supplementary Figure S9). Surprisingly, the *jmj14* mutation promotes flowering time even in the *ft* background (Supplementary Figure S9). The result suggests that the involvement of JMJ14 in flowering time control is at least partially through a FT-independent pathway.

To confirm the function of NAC050/052 in flowering time regulation, we mutated *NAC050* and *NAC052* by the

CRISPR-CAS9 system and obtained a *nac050/052* double mutant (Figure 3G; Supplementary Figure S10A–D) (37), in which a cytosine nucleotide is separately inserted into both *NAC050* and *NAC052* and leads to frame shifts of *NAC050* and *NAC052* (Supplementary Figure S10C and D). As expected, the *nac050/052* double mutant shows an early flowering phenotype relative to the WT (Figure 3G). The effect of *nac050/052* on flowering time is comparable with that of *jmj14*, suggesting that NAC050/052 and JMJ14 are functionally associated in flowering time regulation.

JMJ14 and NAC050/052 regulate a large number of common target genes

To understand the mechanism underlying the collaboration between JMJ14 and NAC050/052, we isolated total RNA from 2-week-old seedlings and performed RNA-seq to identify differentially expressed genes in *jmj14* and *NAC050/052-RNAi* relative to the WT. We obtained in total 3.6×10^7, 1.9×10^7 and 1.2×10^7 reads for WT, *jmj14* and *NAC050/052-RNAi*, respectively. For each of the libraries, at least 80% of the reads are uniquely matched to the *Arabidopsis* genome (Supplementary Table S3). From the RNA-seq analysis, the reads that matched to *JMJ14* were blocked in the *jmj14* mutant, while the reads corresponding to the *NAC050* cDNA fragment in the *NAC050-RNAi* construct were highly accumulated, thereby causing a reduced transcript level of *NAC050* in the *NAC050/052-RNAi* lines (Figure 4A and B). The results suggest that our RNA-seq data are reliable (Supplementary Tables S4 and S5). In addition to *NAC050* and *NC052*, 15 *NAC* genes were differentially expressed in the *NAC50/052-RNAi* lines (Supplementary Table S5). Among the 15 *NAC* genes, 9 genes are increased and 6 genes are decreased. Because the sequences of these differentially expressed *NAC* genes have no sequence similarity with the *NAC050* cDNA fragment used in the *NAC050-RNAi* construct, the expression of these *NAC* genes are likely to be indirectly affected by the *NAC050-RNAi* construct.

The heat map of the differentially expressed genes indicates that the effects of *jmj14* and *NAC050/052-RNAi* on gene expression are highly similar to each other (Figure 4C). A large number of genes are co-upregulated or co-downregulated in the *jmj14* and *NAC050/052-RNAi* plants. We identified 938 and 1470 genes that are significantly upregulated in the *jmj14* and *NAC050/052-RNAi* plants, respectively ($P < 0.01$ and log2 (fold change of reads) > 0.5). More than half (494/938, 52.7%) of the 938 upregulated genes in the *jmj14* mutant overlap with the 1470 upregulated genes in the *NAC050/052-RNAi* plants (Figure 4D; Supplementary Tables S4 and S5). Of the 389 downregulated genes in *jmj14*, nearly half (192/389, 49.4%) overlap with the 1559 downregulated genes in *NAC050/052-RNAi* (Figure 4D; Supplementary Tables S4 and S5). In *jmj14* and *NAC050/052-RNAi*, the expected numbers for overlapping upregulated and downregulated genes by chance are 40 and 18, respectively. The numbers are significantly less than those of observed overlapping genes, suggesting a functional association between JMJ14 and NAC050/052. To confirm the effect of *jmj14* and *NAC050/052-RNAi* on co-upregulated genes as determined by RNA-seq, we selected 10 of them for validation by quantitative RT-PCR (Figure 4E). We found that all the 10 genes are also co-upregulated in our quantitative RT-PCR results (Figure 4F), confirming the RNA-seq data. Moreover, we determined whether co-upregulated genes identified in 2-week-old seedlings as determined by RNA-seq are also upregulated in tissues of adult plants. We found that three co-upregulated genes identified in 2-week-old seedlings are markedly upregulated by *jmj14* in all the tested tissues from 1-month-old plants, and the effect of *NAC050/052-RNAi* on the expression of these genes is variable in different tissues (Supplementary Figure S11). In general, *NAC050/052-RNAi* either does not affect their expression in all the tested tissues or affects in some specific tissues to various extents, suggesting that the involvement of JMJ14 in repression of these genes may occur in both NAC050/052-dependent and NAC050/052-independent manners. The expression of JMJ14 target genes are prone to be ubiquitously regulated by JMJ14, whereas the function of NAC050/052 is likely dependent on specific target loci, developmental stages and tissues.

JMJ14 and NAC050/052 are required for the H3K4 demethylation of their common target genes

JMJ14 is a histone H3K4 demethylase that is required for removing H3K4 trimethylation, a histone modification that is related to transcriptional activation (16). We performed H3K4me3 ChIP-seq to determine whether the effect of *jmj14* and *NAC050/052-RNAi* on gene expression is related to H3K4me3. The results show that H3K4me3 is preferentially present in euchromatic regions of each chromosome (Supplementary Figure S12A–E). H3K4me3 plot indicates that H3K4me3 is enriched at 5′-ends of transcribed regions following the transcription start site (Supplementary Figure S12F), which is consistent with previous studies (33,34).

Generally, *jmj14* and *NAC050/052-RNAi* have no significant effect on H3K4me3 at the whole genome level (Supplementary Figure S12A–F). However, we identified in total 555 genes that showed a significantly increased H3K4me3 in *jmj14*, whereas only 62 genes show decreased H3K4me3 (Supplementary Tables S6 and S7), which is consistent with the role of JMJ14 in H3K4 demethylation (13,16,17). At least some of the identified 555 genes may be direct targets of JMJ14, whereas the decrease of H3K4me3 in the 62 genes is likely due to an indirect effect of *jmj14* on gene repression. In the 555 H3K4me3 hypermethylated genes, 130 genes overlap with the 938 genes that are upregulated in *jmj14* (Figure 5A). The overlap is significantly ($P < 0.01$) higher than expected by chance. Simultaneously, only 5 of the H3K4me3 hypermethylation genes overlap with the 389 downregulated genes (Figure 5B). Several previous reports suggest that JMJ14 is a JmjC-type histone H3K4me3 demethylase (13,16,17). It is likely that the change of H3K4me3 levels in *jmj14* as well as in the RNAi lines of its related NAC proteins is directly caused by the reduced action of JMJ14. However, we cannot rule out the possibility that the change in H3K4me3 reflects an indirect effect of gene expression.

For 494 co-upregulated genes in *jmj14* and *NAC050/052-RNAi* plants, the effect of *jmj14* and *NAC050/052-RNAi*

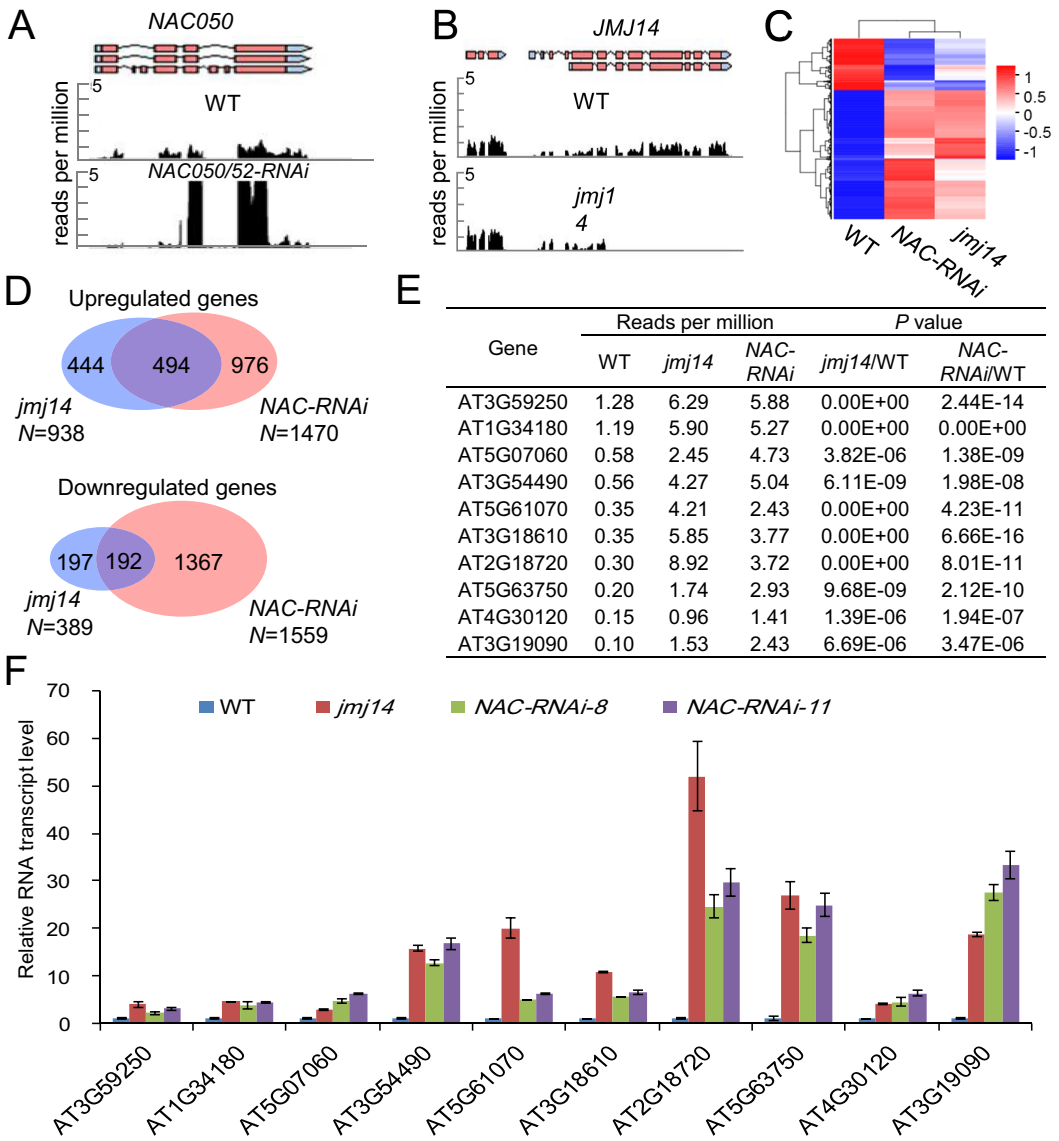

Gene	Reads per million			*P* value	
	WT	*jmj14*	*NAC-RNAi*	*jmj14*/WT	*NAC-RNAi*/WT
AT3G59250	1.28	6.29	5.88	0.00E+00	2.44E-14
AT1G34180	1.19	5.90	5.27	0.00E+00	0.00E+00
AT5G07060	0.58	2.45	4.73	3.82E-06	1.38E-09
AT3G54490	0.56	4.27	5.04	6.11E-09	1.98E-08
AT5G61070	0.35	4.21	2.43	0.00E+00	4.23E-11
AT3G18610	0.35	5.85	3.77	0.00E+00	6.66E-16
AT2G18720	0.30	8.92	3.72	0.00E+00	8.01E-11
AT5G63750	0.20	1.74	2.93	9.68E-09	2.12E-10
AT4G30120	0.15	0.96	1.41	1.39E-06	1.94E-07
AT3G19090	0.10	1.53	2.43	6.69E-06	3.47E-06

Figure 4. Effect of *jmj14* and *NAC050/052-RNAi* on gene expression as determined by RNA-seq. (A) The plots show the RNA reads that matched *NAC050* and *NAC052*. The RNA reads were plotted in the WT and *NAC050/052-RNAi* plants. (B) The *JMJ14* RNA reads were plotted in the WT and *jmj14* plants. RNA reads of a flanking gene are comparable between the WT and *jmj14* plants and are shown as a control. (C) Heat map of differentially expressed genes in *jmj14* and *NAC-RNAi* plants relative to the WT. (D) Venn diagram showing the overlap of differentially expressed genes in *jmj14* and *NAC-RNAi* plants. (E) Showing is the list of co-upregulated genes that were selected for quantitative RT-PCR assay. Normalized reads in each ecotype and *P*-values are indicated. (F) Quantitative RT-PCR was performed to confirm the effect of *jmj14* and *NAC050/052-RNAi* on the expression of their target genes as determined by RNA-seq. Two individual *NAC050/052-RNAi* lines, 8 and 11, were used. The expression of the actin gene was used as an internal control. The results of three technical replicates were shown. Total RNA used for RNA-seq and quantitative RT-PCR was extracted from 2-week-old seedlings.

on gene expression is comparable (Figure 5C), but the H3K4me3 level is increased in *jmj14* and to a lesser extent in *NAC050/052-RNAi* plants (Figure 5D). The results suggest that NAC050 and NAC052 are involved in transcriptional repression through both histone demethylation-dependent and demethylation-independent pathways. To confirm the H3K4me3 ChIP-seq data, we selected some H3K4me3 hypermethylated genes for validation by ChIP-PCR (Figure 5E). Only those genes with a long intergenic region (>1 kb) were selected to exclude the influence of upstream genes. Consistent with the H3K4me3 ChIP-seq data (Figure 5D), our quantitative ChIP-PCR results indicate that *jmj14* and *NAC050/052-RNAi* derepress H3K4me3 at 5′-ends of transcribed regions but not at intergenic regions (Figure 5E; Supplementary Table S1).

In our H3K4me3 ChIP-seq results, a number of up-regulated genes in *jmj14* and *NAC050/052-RNAi* were not identified as being H3K4me3 hypermethylated (Figure 5A). We randomly selected six of these genes and determined their H3K4me3 levels by H3K4me3 ChIP-PCR. The results indicate that the H3K4me3 levels of the six genes are more or less increased in *jmj14* and to a lesser ex-

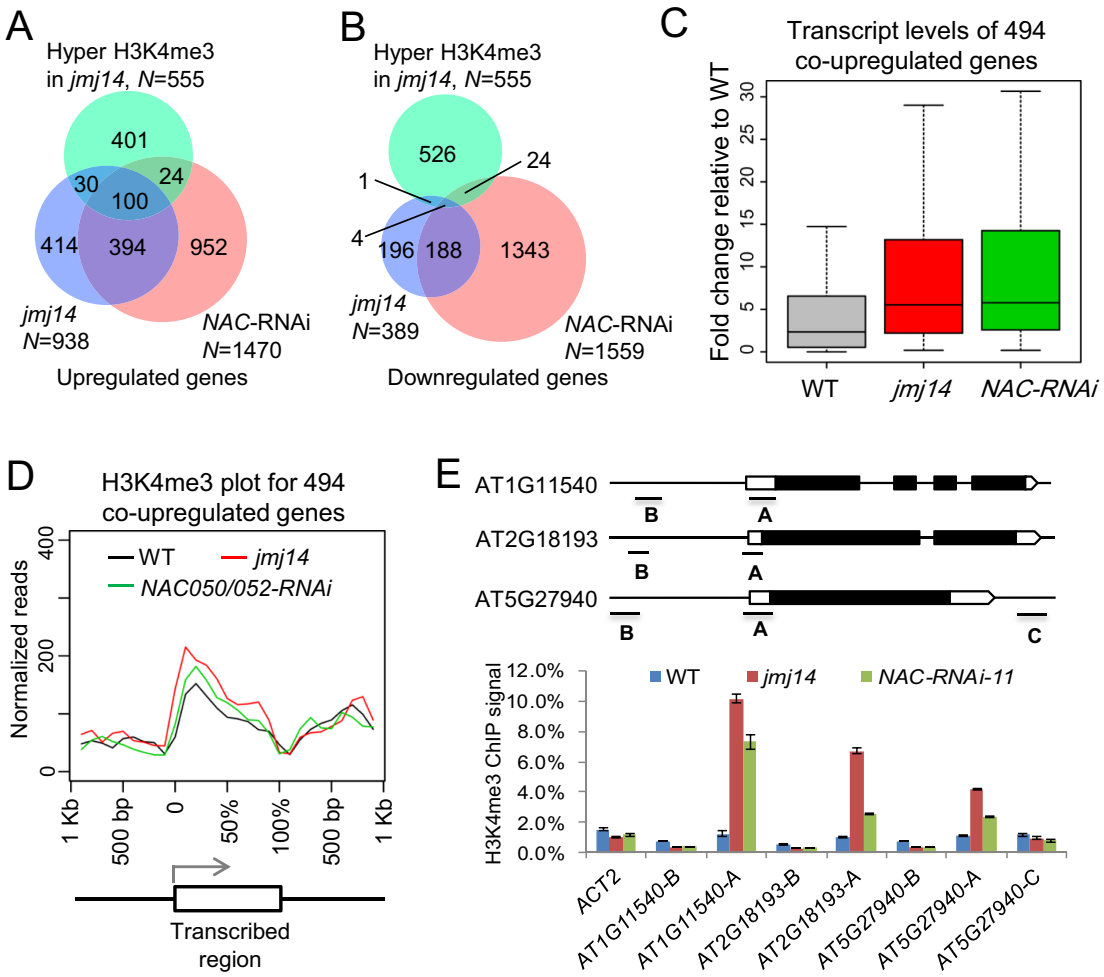

Figure 5. Effect of *jmj14* and *NAC050/052-RNAi* on H3K4me3 as determined by ChIP-seq. (A and B) Venn diagrams showing the overlap between the H3K4me3 hypermethylated genes in *jmj14* and the upregulated (A) or downregulated genes (B) in *jmj14* and *NAC050/052-RNAi* plants. (C) Box plot showing the effect of *jmj14* and *NAC050/052-RNAi* on gene expression for 494 co-upregulated genes in *jmj14* and *nac050/052-RNAi*. (D) H3K4me3 of the 494 overlapping upregulated genes in *jmj14* and *NAC050/052-RNAi* plants was plotted for the transcription regions along with the 1-kb upstream and downstream flanking regions. The *y*-axis indicates the normalized reads number. (E) H3K4me3 hypermethylated genes identified by ChIP-seq were confirmed by ChIP-PCR in the WT, *jmj14* and *NAC050/052-RNAi* plants. Diagrams show positions of all DNA fragments amplified in the ChIP-PCR assay. The hypermethylated sites include *AT1G11540-A*, *AT2G18193-A* and *AT5G27940-A*. The sites that are adjacent to the H3K4me3 hypermethylated regions were used as negative controls. These sites are *AT1G11540-B*, *AT2G18193-B*, *AT5G27940-B* and *AT5G27940-C*. Two-week-old seedlings were used for ChIP-seq and ChIP-PCR.

tent in *NAC050/052-RNAi* (Supplementary Figures S13 and S14). The results suggest that the effect of *jmj14* and *NAC050/052-RNAi* on H3K4me3 was undervalued in our H3K4me3 ChIP-seq results and that JMJ14 and NAC050/052 are probably required for histone H3K4 demethylation in majority of their common target genes.

JMJ14 and NAC050/052 directly bind their common target genes and act in transcriptional repression

We performed quantitative ChIP-PCR for *JMJ14* to determine whether JMJ14 directly binds its target genes. The construct harboring the native promoter-driven *JMJ14–3xFlag* transgene was equivalently expressed in WT and *NAC050/052-RNAi* plants (Supplementary Figure S15A). The occupancy of JMJ14–3xFlag on transcription start sites was determined by ChIP-PCR using anti-Flag antibody-conjugated agarose beads. Genes that were upregulated in both *jmj14* and *NAC050/052-RNAi* were hypothesized to be the common targets of JMJ14 and NAC050/052 and were selected for ChIP-PCR (Figures 4D and 6A; Supplementary Tables S4 and S5). We found that JMJ14 is enriched at the transcription start sites of the common target genes in the WT background, indicating that these genes are direct targets of JMJ14, whereas JMJ14 is not enriched at the transcription start sites of the control genes *ACT2* and *AT1G02580* whose expression is not affected by *jmj14* (Figure 6A; Supplementary Figure S13). Moreover, we found that the enrichment of JMJ14 on these genes is not significantly affected in the *NAC050/052-RNAi* plants (Figure 6A; Supplementary Figure S13), suggesting that NAC050/052 have no effect on the occupancy of JMJ14 on chromatin.

We performed an NAC050 ChIP-PCR assay to determine whether NAC050 directly binds to the target loci

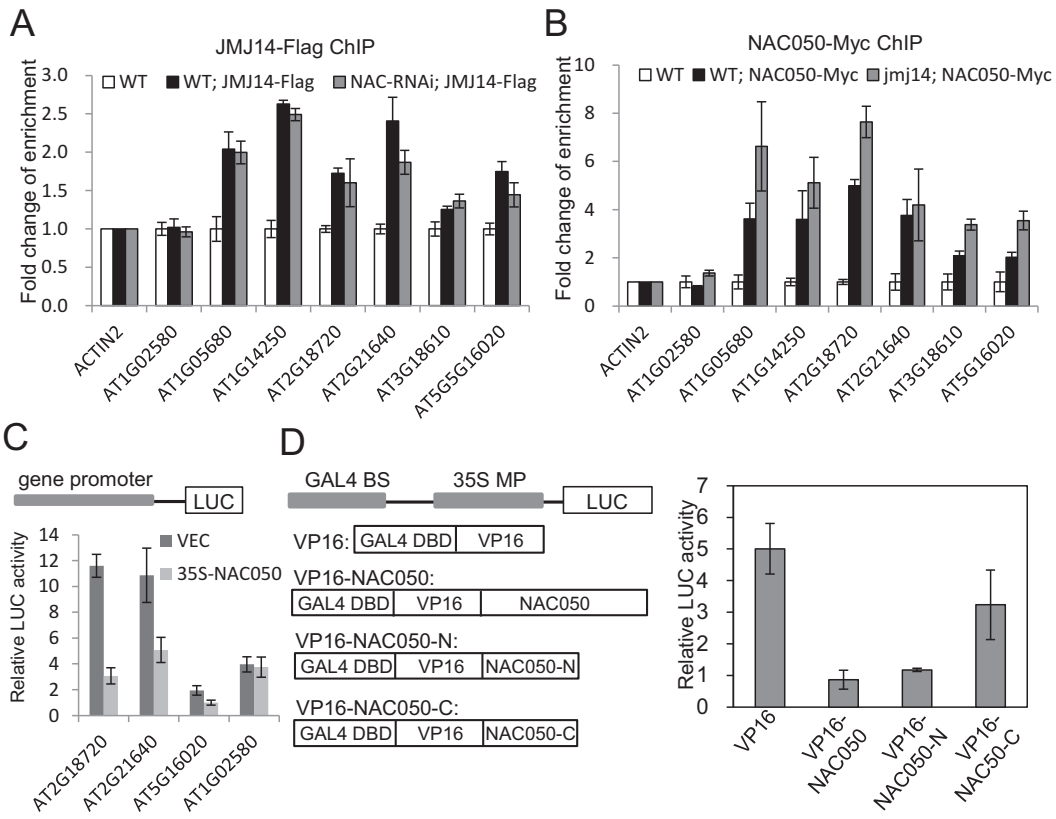

Figure 6. JMJ14 and NAC050 bind to their common target genes. (A) JMJ14-Flag ChIP-PCR was performed to determine the occupancy of JMJ14-Flag at the common targets of JMJ14 and NAC050/052. The *JMJ14–3xFlag* construct was transformed and stably expressed in the WT as well as in *NAC050/052-RNAi* plants. (B) NAC050-Myc ChIP-PCR was performed to examine the occupancy of NAC050–3xMyc at the common targets of JMJ14 and NAC050/052. The *NAC050–3xMyc* construct was introduced into the WT and *jmj14* plants. The expression levels of *NAC050–3xMyc* in the WT and *jmj14* plants are equivalent. Two-week-old seedlings of each genotype were used in the ChIP-PCR assay for JMJ14-Flag and NAC-Myc. (C) The transcriptional repression activity of NAC050 was determined by the transient expression of the luciferase reporter in protoplast cells. The luciferase reporter gene was driven by the promoter sequences of *AT2G18720*, *AT2G21640*, *AT5G16020* and *AT1G02580*. The *35S-NAC050* construct was transformed to determine whether the overexpression of *NAC050* represses the luciferase activity. (D) The luciferase reporter gene was driven by the minimal *35S* promoter with the upstream GAL4-binding site. In the effector construct, the transcriptional activator VP16 fused to the GAL4 DNA-binding domain activates the transcription of the reporter gene. Either the full-length *NAC050* or truncated *NAC* sequences were ligated in frame with the *GAL4-VP16* fusion sequence in the effector construct. The reporter construct and each of the effector constructs were co-transformed into protoplast cells for the luciferase activity assay. The experiments in this figure were biologically repeated and the same results were obtained. Showing is the results of three technical replicates from a representative experiment.

that are shared by JMJ14 and NAC050/052. The *NAC050–3xMyc* construct was transformed and expressed in WT and *jmj14* plants (Supplementary Figure S15B). The ChIP-PCR results indicate that NAC050 is significantly enriched at the common target genes that are shared by JMJ14 and NAC050/052 but not at *ACT2* and *AT1G02580* (Figure 6B), suggesting that these common target genes are the direct targets of NAC050. The enrichment of NAC050 at these loci was not decreased in the *jmj14* mutant (Figure 6B), implying that JMJ14 is not required for the occupancy of NAC050 on its target loci. These results suggest that JMJ14 and NAC050 are recruited to their common target genes independently. The aforementioned results indicated that the FYRC domain of JMJ14 is responsible for the interaction of JMJ14 with NAC050 (Figure 2B–D). We determined whether the FYRC domain is required for the function of JMJ14 in transcriptional repression by a complementation assay. *AT3G18610* and *AT3G59250* are two common target genes shared by NAC050/052 and JMJ14. In the *jmj14* mutant and the *NAC050/052-RNAi* lines, the expression of the two genes is significantly upregulated (Supplementary Tables S4 and S5; Figure 4E and F). By the complementation assay, we demonstrated that the expression of the two genes in the *jmj14* mutant was restored by the full-length transgene *JMJ14-Flag* but not by the truncated transgene *JMJ14-a-Flag* in which the FYRC domain is absent (Supplementary Figure S16). Although the recruitment of JMJ14 to its target genes is independent of NAC050, the interaction of NAC050 with JMJ14 may contribute to the function of JMJ14 on its target loci. However, we cannot absolutely exclude the possibility that the FYRC domain has another function, which is probably responsible for the loss-of-function phenotype. The *NAC050/052-RNAi* lines exhibit elevated H3K4me3 levels at the common target genes shared by NAC050/NAC052 and JMJ14 (Figure 5D and E; Supplementary Figures S13 and S14). It

is difficult to rule out the possibility that the elevation of H3K4me3 is caused by increased transcript levels, but the physical and functional association between NAC050/052 and JMJ14 strongly suggests that NAC050/052 directly regulate the function of the histone demethylase JMJ14 at their common target genes.

JMJ14 acts as a H3K4 demethylase and is involved in transcriptional repression (15–18). NAC050 directly binds the common target genes of NAC050 and JMJ14 and represses the expression of these genes (Figure 6B; Supplementary Table S5), suggesting that NAC050 can act as a transcriptional repressor of these genes. *AT2G18720*, *AT2G21640* and *AT5G16020* are the common target genes shared by JMJ14 and NAC050/052 (Supplementary Tables S4 and S5; Figure 6A and B). The promoter sequences of these genes were used to drive the luciferase reporter gene in a transient expression assay in protoplast cells (Figure 6C). While their promoter sequences drive the expression of the luciferase reporter gene, the transformation of the construct harboring the *35S-NAC050* overexpression construct significantly reduces the expression of the reporter gene (Figure 6C). The expression of *AT1G02580* was not affected by *NAC050/052-RNAi* (Supplementary Table S5), and its promoter had no predicted NAC050-binding site and failed to be bound by NAC050 (Figure 6B). Thus, we used the promoter of *AT1G02580* as a negative control in the luciferase reporter assay. As expected, we found that the luciferase reporter driven by the promoter of *AT1G02580* was not affected by overexpression of *NAC050* (Figure 6C). These results suggest that NAC050 acts as a transcriptional repressor on its target genes.

We further performed a reporter gene assay using the luciferase reporter gene driven by a minimum *35S* promoter with a GAL4 binding site *5xUAS* (Figure 6D). In the effector construct, the full-length or truncated NAC050 coding sequences were ligated in frame with the coding sequence of the GAL4 DBD-VP16 fusion protein, in which the GAL4 DNA binding domain was fused with the VP16 transcriptional activation domain. As previously reported, GAL4 DBD-VP16 by itself activates the expression of the luciferase reporter gene (Figure 6D). When either the full-length NAC050 or the N-terminal half of NAC050 was fused with GAL4 DBD-VP16 in the effector construct, the reporter gene expression was markedly decreased (Figure 6D). However, when the C-terminal half of NAC050 was fused with GAL4 DBD-VP16, the reporter gene expression was only weakly affected (Figure 6D). Thus, NAC050 is a transcription repressor and the transcriptional repression domain is included in the N-terminal region of NAC050. A previous study identified a conserved transcriptional repression domain (NARD) at the N-terminal region of NAC transcription factors (39). We found that the NARD domain is conserved at the N-terminal region of NAC050, which is consistent with the requirement of the N-terminal region of NAC050 for transcriptional repression (Figure 6D).

Identification of NAC050-binding DNA elements

We have demonstrated that NAC050 is recruited to its target genes independently of JMJ14 (Figure 6B). It is interesting to identify the DNA cis-element that is bound by NAC050/052. As described above, *UGT74E2* (AT1G05680) is a common target gene that is shared by NAC050/052 and JMJ14 (Figure 6A and B; Supplementary Tables S4 and S5). An EMSA indicated that the bacterially expressed GST-NAC050 and GST-NAC052 can bind the ∼300-bp promoter sequence (P1) of *UGT74E2* (Supplementary Figure S17A and B). In NAC050, the N-terminal NAC domain but not the C-terminal regulatory domain is responsible for the DNA-binding ability (Supplementary Figure S17C). Therefore, we used the NAC domain protein in EMSA to determine the NAC050-binding DNA element in the *UGT74E2* promoter sequence. The NAC domain of NAC050 not only binds to the ∼300-bp *UGT74E2* promoter sequence (P1), but also binds to the truncated sequence (P2) from −194 to +13 (Figure 7A; Supplementary Figure S17A). Seven individual oligonucleotides (P3–P9) covering the full-length P2 sequence were used in the EMSA to identify the fragments that are required for NAC050 binding (Figure 7A; Supplementary Figure S17). The results indicate that only the oligonucleotides P8 and P9 can be bound by NAC050 (Figure 7A).

To determine the NAC050-binding DNA element in the P9 sequence of the *UGT74E2* promoter, we generated a series of mutant P9 oligonucleotides harboring mutations in three residues and performed EMSA (Figure 7B). The binding of NAC050 to the mutant P9 sequences was normalized by the binding of NAC050 to the WT P9 sequence. The results indicate that the binding of NAC050 to the mutant P9 oligonucleotide P9-M7 was significantly reduced compared to the binding of NAC050 to the WT P9 oligonucleotide (Figure 7B), suggesting that the mutation site in P9-M7 is required for the binding of NAC050. We thereafter generated a series of mutant P9 oligonucleotides harboring mononucleotide mutations covering the mutant site of P9-M7 (Figure 7C). The EMSA demonstrated that the CACG motif in P9 is sufficient for the binding of NAC050 (Figure 7C). In the CACG motif, the first and third cytosines can be substituted by thymine and adenine, respectively, without affecting the binding of NAC050, while other substitutions reduce the binding (Figure 7C). Thus, the optimal NAC050-binding motif is (C/T)A(C/A)G. This motif is absent in the five other tested oligonucleotides P3, P4, P5, P6 and P7, which is consistent with the defect in the binding of NAC050 to these oligonucleotides (Figure 7A; Supplementary Figure S17A). However, although the canonical NAC050-binding motif is absent in P8, NAC050 can still bind to P8 (Figure 7A; Supplementary Figure S17A). The sequence of P8 is CAATTTTTGGATTGTAGTCCAATTAATGAG and its reverse-complement sequence is CTCATTAATTGGACTACAATCCAAAAATTG (Supplementary Figure S17A). The underlined DNA sequences are weak NAC050-binding motifs as determined by our EMSA experiment (Figure 7C). There are totally seven weak NAC050-binding motifs in P8, suggesting that the presence of a high number of weak NAC050-binding motifs is probably sufficient for binding.

To confirm that the identified NAC050-binding element is functional, we integrated five repeats of the NAC050-binding element into the promoter of the luciferase reporter

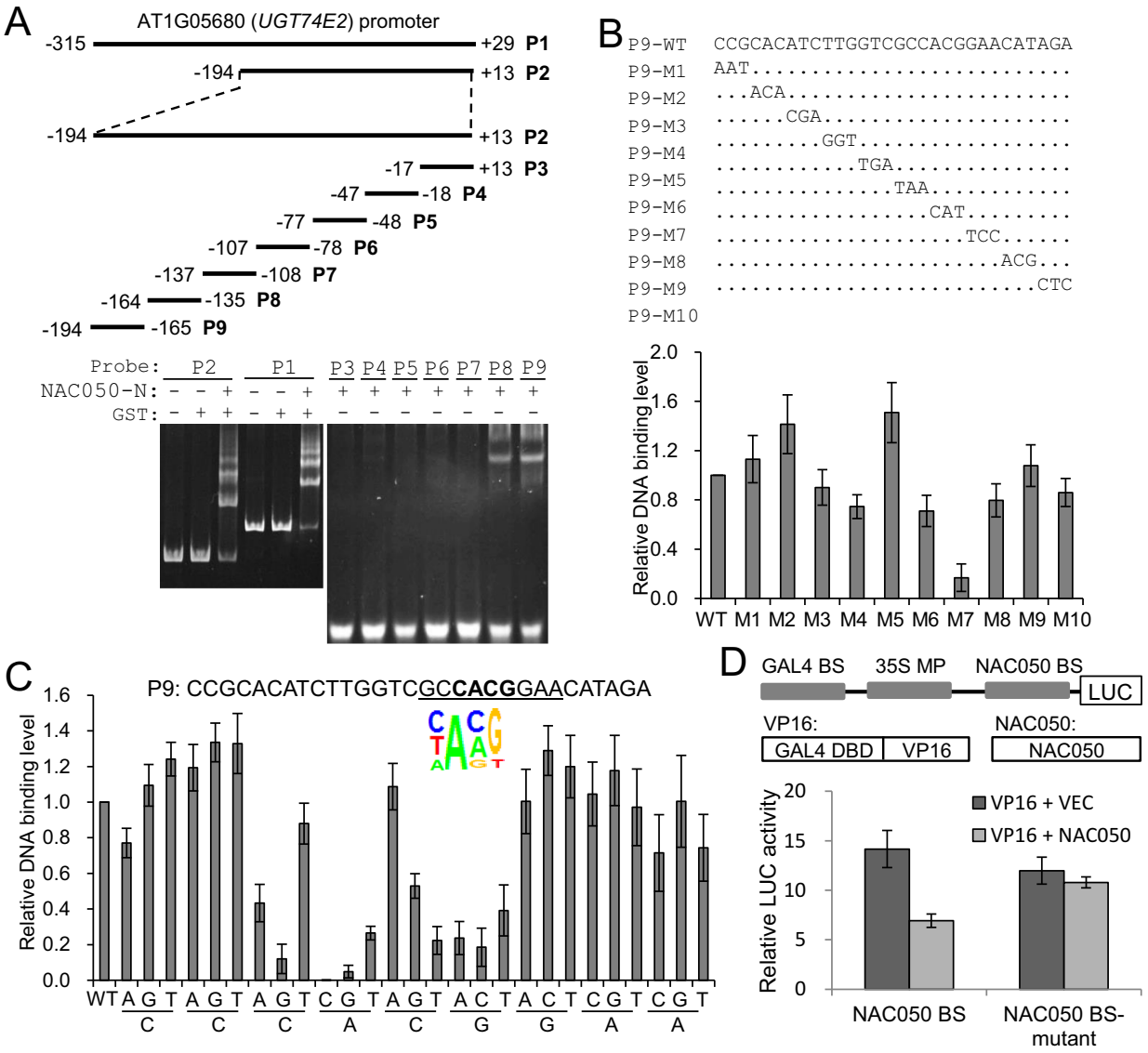

Figure 7. Identification and characterization of the NAC050/052-binding DNA cis-element. (A) NAC050 binds to the promoter sequence of its target gene *UGT74E2* as determined by EMSA. A series of DNA fragments in the AT1G05680 promoter were used in the binding assay. (B) The oligonucleotide sequence AT1G05680-P9 harboring the NAC050 binding site was mutated at a series of three nucleotides and then used in the NAC050 binding assay. The binding levels were normalized by the binding between NAC050 and the WT oligonucleotide sequence. Shown are the results from three independent replicates. (C) The AT1G05680-P9 oligonucleotide was subjected to mutation at one residue and was then used in the NAC050 binding assay by EMSA. Each nucleotide was mutated to three other nucleotides to determine the alternation of the nucleotide. (D) The luciferase reporter gene was driven by the *35S* minimal promoter ligated with GAL4 binding element in front of a 5xNAC050-binding element (CTTGGTCGCCACGGAA). The 5xNAC050-binding element was substituted with CTTGGTCGCCCCGGAA and used as a negative control. The expression of the reporter gene was determined by the luciferase activity assay in protoplast cells. The effector construct GAL4-DBD-VP16 was used to activate the reporter gene. The *NAC050* expression construct was transformed to determine the effect of NAC050 on the expression of the reporter gene.

gene, which contains a *35S* minimal promoter and a GAL4 binding site (Figure 7D). The luciferase reporter gene was transiently expressed in protoplast cells, whereas NAC050 overexpression inhibited ~50% of the luciferase reporter gene expression (Figure 7D). However, when the NAC050-binding element repeats were mutated, NAC050 overexpression failed to inhibit the expression of the reporter gene (Figure 7D). The results demonstrate that NAC050 directly binds to the NAC050-binding element repeats and acts as a transcriptional repressor.

We performed an informatic analysis to search for overpresented DNA elements at the promoters of the 494 common target genes shared by JMJ14 and NAC050 (Supplementary Tables S4 and S5; Figure 4D), and found that the DNA element containing CACG is the most enriched DNA element at the promoters of these genes (Supplementary Figure S18). These results suggest that the NAC050-binding DNA element identified in this study is predictive and is a functional NAC050-binding DNA element *in vivo*.

DISCUSSION

The physical and functional links between JmjC histone demethylases and transcription factors have been well studied in mammals (22–24). It is important to determine whether and how JmjC histone demethylases associate with transcription factors in plants. NAC transcription factors form one of the largest transcription factor families in plants and are involved in diverse biological processes (26,27). We demonstrate that JMJ14 is involved in flowering time regulation by associating with two previously uncharacterized NAC transcription repressors NAC050 and NAC052. The NAC family proteins contain a conserved NAC domain that is responsible for DNA binding (40). Although the NAC domains are conserved in different subgroups of the NAC family proteins, their DNA recognition sequences are diverse (28,40–42). We identified a NAC050-binding DNA element in the promoter of the NAC050/052 target gene (AT1G05680), demonstrating that (C/T)A(C/A)G is the optimal NAC050 recognition motif (Figure 7), which is similar to the previously identified CACG motif that is bound by NAC019, NAC055 and NAC072 (40). We propose that in addition to the NAC050/052-binding element, other characteristics of chromatin are probably required for NAC050/052 recognition of chromatin.

JMJ14 is a histone H3K4 demethylase that is involved in the demethylation of H3K4 concomitantly with repression of gene transcription (15–18). We demonstrate that JMJ14 is physically associated *in vivo* with the two NAC proteins NAC050 and NAC052 (Figures 1 and 2), which is consistent with the finding of the interaction between JMJ14 and NAC050 in a proteome-wide yeast two-hybrid assay for *Arabidopsis* (43). More importantly, we confirm the functional association between JMJ14 and NAC050/052 in flowering time control (Figure 3A–G). RNA-seq identified a number of genes that are increased in either *jmj14* or *NAC050/052-RNAi*, with more than half of the increased genes in *jmj14* overlapping with those in *NAC050/052-RNAi* (Figure 4C and D). These results demonstrate a functional link between JMJ14 and NAC050/052. Previous studies demonstrated that the early flowering phenotype of *jmj14* is correlated with increased expression of floral integrator genes (13,16,17), which are consistent with our study (Figure 3E). We found that the expression of the floral integrator genes *FT*, *LFY* and *PI* is also increased in the two individual *NAC050/052-RNAi* lines (Figure 3E), which is consistent with the fact that the expression of a large number of genes is increased by both *jmj14* and *NAC050/052-RNAi* in our RNA-seq results (Figure 4C and D; Supplementary Tables S4 and S5). Moreover, the expression of the floral integrator genes *FT* and *PI* is decreased in the *NAC050* overexpression plants (Figure 3E), confirming that NAC050 is involved in the repression of floral integrator genes. The early flowering phenotype that is shared by *jmj14* and *NAC050/052-RNAi* is related to the depression of their common target floral integrator genes.

Histone H3K4 methylation is predominantly enriched at the transcription start sites of two-thirds of the protein-coding genes in the *Arabidopsis* genome (33,34). H3K4 methylation is usually correlated with actively transcribed genes (33). The SET domain-containing histone H3K4 methyltransferases ATX1, EFS/SDG8 and ATXR7/SDG25 are responsible for H3K4 methylation at the flowering repressor gene *FLC*. The *atx1*, *efs/sdg8* and *atxr7/sdg25* mutants present an early flowering phenotype that is accompanied by decreased H3K4 trimethylation at *FLC* (44–46). FLD, a homolog of the human histone H3K4 demethylase LSD1, is involved in the H3K4 demethylation of *FLC* and is therefore responsible for the repression of *FLC* (47–49). The histone H3K4 methylation activity of EFS/SDG8 is antagonized by the H3K4 demethylation activity of FLD at *FLC* (14). The JmjC-type histone demethylases JMJ15 and JMJ18 are also involved in H3K4 demethylation at *FLC* (14,20,21). Thus, histone H3K4 methylation and demethylation at *FLC* play important roles in flowering time regulation.

Although JMJ14 is a histone H3K4 demethylase that shows a high degree of similarity to JMJ15 and JMJ18 (15), JMJ14 can specifically repress floral integrator genes, but not the floral repressor gene *FLC*, that are targeted by JMJ15 and JMJ18. Thus, JMJ14 acts as a floral repressor (15–18), which is in contrast to the floral integrator role of JMJ15 and JMJ18 (20,21). It is necessary to understand how histone demethylases act on their specific target genes.

We demonstrate that JMJ14 specifically cooperates with NAC050/052 and is involved in the repression of a number of common target genes (Figures 1 and 4C and D; Supplementary Tables S4 and S5). Unlike JMJ14, JMJ15 and JMJ18 fail to interact with NAC050/052 (Supplementary Figure S5). The C-terminal FYRC domain of JMJ14 is necessary for the interaction between JMJ14 and NAC050/052 (Figure 2B–D). We found that although the N-terminal region of JMJ14 is highly similar with that of JMJ15 and JMJ18, the C-terminal FYRC domain of JMJ14 is much different from that of JMJ15 and JMJ18 (Supplementary Figure S4). The absence of the FYRC domain in JMJ15 and JMJ18 is consistent with the finding that JMJ15 and JMJ18 fail to interact with NAC050/052 as determined by yeast two-hybrid. JMJ14 and NAC050/052 directly bind their common target genes and act as transcription repressors of these genes (Figure 6A–D; Supplementary Tables S4 and S5). Thus, the functional specificity of JMJ14 in flowering time control is consistent with the interaction specificity of JMJ14 with NAC050/052 on their common target genes. Further studies are required to understand whether the interaction of JMJ14 with NAC050/052 is necessary for the function of JMJ14 in gene regulation and flowering time control.

Our results suggest that the full length of NAC050 is required for the interaction of NAC050 with JMJ14 (Supplementary Figure S6). The N-terminal NAC domain of NAC transcription factors is conserved and is required for NAC dimerization as well as for DNA binding (25). NAC050 and NAC052 not only form dimers but also associate with JMJ14 (Figures 1A–C and 2A). The NAC transcription factors have been demonstrated to bind DNA in the form of dimers (50,51). JMJ14 may interact with NAC050/052 dimers or higher molecular weight oligomers but not with NAC050/052 monomers at their common target genes. Thus, the NAC domain-mediated oligomerization of NAC050/052 is most likely necessary for the inter-

action between NAC050/052 with JMJ14. The C-terminal transcription regulatory domain is diversified in the NAC transcription factors and is necessary for functional specificities of distinct NAC subgroups (25,52). It is possible that the C-terminal transcription regulatory domain is required for the formation of an integral NAC050/052 oligomer structure, thereby facilitating the interaction between NAC050/052 and JMJ14.

It is interesting to understand how JMJ14 and NAC050/052 collaborate in the JMJ14-NAC050/052 complex to transcriptionally repress their common target genes. The H3K4me3 level for co-upregulated genes in *jmj14* and *NAC050/052-RNAi* is not only increased in *jmj14* but also in *NAC050/052-RNAi*, suggesting that NAC050/052 are involved in JMJ14-mediated H3K4 demethylation (Figure 5D and E; Supplementary Figure S14). However, the effect of *NAC050/052-RNAi* on H3K4me3 is much less than that of *jmj14* for co-upregulated genes shared in *jmj14* and *NAC050/052-RNAi* even though the effect of *jmj14* and *NAC050/052-RNAi* on gene expression is comparable (Figure 5C and D). The results suggest that NAC050/052 are involved in transcriptional repression by both H3K4 demethylation-dependent and demethylation-independent pathways. Moreover, we identified a large number of genes that are exclusively upregulated in *NAC050/052-RNAi* but not in *jmj14*, suggesting that NAC050/052 act as a transcription repressor even without JMJ14 (Figure 4C and D; Supplementary Tables S4 and S5). For common target genes shared by NAC050/052 and JMJ14, we propose that NAC050/052 not only acts as a transcription repressor to directly repress Pol II-dependent transcription but also associates with JMJ14 and is probably responsible for enhancing the H3K4 demethylation activity of JMJ14 (Supplementary Figure S19). The integrity of the JMJ14-NAC050/052 complex is necessary for transcriptional repression of these genes. Moreover, JMJ14 represses the expression of *NAC050/052* (Figure 3A; Supplementary Table S4), facilitating a feedback loop between NAC050/052 and JMJ14 in transcriptional repression control (Supplementary Figure S19).

SUPPLEMENTARY DATA

Supplementary Data are available at NAR Online.

FUNDING

National Basic Research Program of China (973 Program) [2012CB910900]; Chinese Ministry of Science and Technology (973 Program) [2011CB812600]. Funding for open access charge: National Basic Research Program of China (973 Program) [2012CB910900]; Chinese Ministry of Science and Technology (973 Program) [2011CB812600].
Conflict of interest statement. None declared.

REFERENCES

1. Baumbusch,L.O., Thorstensen,T., Krauss,V., Fischer,A., Naumann,K., Assalkhou,R., Schulz,I., Reuter,G. and Aalen,R.B. (2001) The Arabidopsis thaliana genome contains at least 29 active genes encoding SET domain proteins that can be assigned to four evolutionarily conserved classes. *Nucleic Acids Res.*, **29**, 4319–4333.
2. Springer,N.M., Napoli,C.A., Selinger,D.A., Pandey,R., Cone,K.C., Chandler,V.L., Kaeppler,H.F. and Kaeppler,S.M. (2003) Comparative analysis of SET domain proteins in maize and Arabidopsis reveals multiple duplications preceding the divergence of monocots and dicots. *Plant Physiol.*, **132**, 907–925.
3. Tsukada,Y., Fang,J., Erdjument-Bromage,H., Warren,M.E., Borchers,C.H., Tempst,P. and Zhang,Y. (2006) Histone demethylation by a family of JmjC domain-containing proteins. *Nature*, **439**, 811–816.
4. Pedersen,M.T. and Helin,K. (2010) Histone demethylases in development and disease. *Trends Cell Biol.*, **20**, 662–671.
5. Lu,F., Li,G., Cui,X., Liu,C., Wang,X.J. and Cao,X. (2008) Comparative analysis of JmjC domain-containing proteins reveals the potential histone demethylases in Arabidopsis and rice. *Jo. Integr. Plant Biol.*, **50**, 886–896.
6. Chen,X., Hu,Y. and Zhou,D.X. (2011) Epigenetic gene regulation by plant Jumonji group of histone demethylase. *Biochim. Biophys. Acta*, **1809**, 421–426.
7. Saze,H., Shiraishi,A., Miura,A. and Kakutani,T. (2008) Control of genic DNA methylation by a jmjC domain-containing protein in Arabidopsis thaliana. *Science*, **319**, 462–465.
8. Miura,A., Nakamura,M., Inagaki,S., Kobayashi,A., Saze,H. and Kakutani,T. (2009) An Arabidopsis jmjC domain protein protects transcribed genes from DNA methylation at CHG sites. *EMBO J.*, **28**, 1078–1086.
9. Inagaki,S., Miura-Kamio,A., Nakamura,Y., Lu,F., Cui,X., Cao,X., Kimura,H., Saze,H. and Kakutani,T. (2010) Autocatalytic differentiation of epigenetic modifications within the Arabidopsis genome. *EMBO J.*, **29**, 3496–3506.
10. Jones,M.A., Covington,M.F., DiTacchio,L., Vollmers,C., Panda,S. and Harmer,S.L. (2010) Jumonji domain protein JMJD5 functions in both the plant and human circadian systems. *Proc. Natl. Acad. Sci. U.S.A.*, **107**, 21623–21628.
11. Lu,S.X., Knowles,S.M., Webb,C.J., Celaya,R.B., Cha,C., Siu,J.P. and Tobin,E.M. (2011) The Jumonji C domain-containing protein JMJ30 regulates period length in the Arabidopsis circadian clock. *Plant Physiol.*, **155**, 906–915.
12. Cho,J.N., Ryu,J.Y., Jeong,Y.M., Park,J., Song,J.J., Amasino,R.M., Noh,B. and Noh,Y.S. (2012) Control of seed germination by light-induced histone arginine demethylation activity. *Dev. Cell*, **22**, 736–748.
13. Jeong,J.H., Song,H.R., Ko,J.H., Jeong,Y.M., Kwon,Y.E., Seol,J.H., Amasino,R.M., Noh,B. and Noh,Y.S. (2009) Repression of FLOWERING LOCUS T chromatin by functionally redundant histone H3 lysine 4 demethylases in Arabidopsis. *PloS ONE*, **4**, e8033.
14. Ko,J.H., Mitina,I., Tamada,Y., Hyun,Y., Choi,Y., Amasino,R.M., Noh,B. and Noh,Y.S. (2010) Growth habit determination by the balance of histone methylation activities in Arabidopsis. *EMBO J.*, **29**, 3208–3215.
15. Searle,I.R., Pontes,O., Melnyk,C.W., Smith,L.M. and Baulcombe,D.C. (2010) JMJ14, a JmjC domain protein, is required for RNA silencing and cell-to-cell movement of an RNA silencing signal in Arabidopsis. *Genes Dev.*, **24**, 986–991.
16. Lu,F., Cui,X., Zhang,S., Liu,C. and Cao,X. (2010) JMJ14 is an H3K4 demethylase regulating flowering time in Arabidopsis. *Cell Res.*, **20**, 387–390.
17. Yang,W., Jiang,D., Jiang,J. and He,Y. (2010) A plant-specific histone H3 lysine 4 demethylase represses the floral transition in Arabidopsis. *Plant J.*, **62**, 663–673.
18. Deleris,A., Greenberg,M.V., Ausin,I., Law,R.W., Moissiard,G., Schubert,D. and Jacobsen,S.E. (2010) Involvement of a Jumonji-C domain-containing histone demethylase in DRM2-mediated maintenance of DNA methylation. *EMBO Rep.*, **11**, 950–955.
19. Le Masson,I., Jauvion,V., Bouteiller,N., Rivard,M., Elmayan,T. and Vaucheret,H. (2012) Mutations in the Arabidopsis H3K4me2/3 demethylase JMJ14 suppress posttranscriptional gene silencing by decreasing transgene transcription. *Plant Cell*, **24**, 3603–3612.
20. Yang,H., Han,Z., Cao,Y., Fan,D., Li,H., Mo,H., Feng,Y., Liu,L., Wang,Z., Yue,Y. *et al.* (2012) A companion cell-dominant and developmentally regulated H3K4 demethylase controls flowering time in Arabidopsis via the repression of FLC expression. *PLoS Genet.*, **8**, e1002664.

21. Yang,H., Mo,H., Fan,D., Cao,Y., Cui,S. and Ma,L. (2012) Overexpression of a histone H3K4 demethylase, JMJ15, accelerates flowering time in Arabidopsis. *Plant Cell Rep.*, **31**, 1297–1308.
22. Yamane,K., Toumazou,C., Tsukada,Y., Erdjument-Bromage,H., Tempst,P., Wong,J. and Zhang,Y. (2006) JHDM2A, a JmjC-containing H3K9 demethylase, facilitates transcription activation by androgen receptor. *Cell*, **125**, 483–495.
23. Tahiliani,M., Mei,P., Fang,R., Leonor,T., Rutenberg,M., Shimizu,F., Li,J., Rao,A. and Shi,Y. (2007) The histone H3K4 demethylase SMCX links REST target genes to X-linked mental retardation. *Nature*, **447**, 601–605.
24. DiTacchio,L., Le,H.D., Vollmers,C., Hatori,M., Witcher,M., Secombe,J. and Panda,S. (2011) Histone lysine demethylase JARID1a activates CLOCK-BMAL1 and influences the circadian clock. *Science*, **333**, 1881–1885.
25. Olsen,A.N., Ernst,H.A., Leggio,L.L. and Skriver,K. (2005) NAC transcription factors: structurally distinct, functionally diverse. *Trends Plant Sci.*, **10**, 79–87.
26. Nakashima,K., Takasaki,H., Mizoi,J., Shinozaki,K. and Yamaguchi-Shinozaki,K. (2012) NAC transcription factors in plant abiotic stress responses. *Biochim. Biophys. Acta*, **1819**, 97–103.
27. Puranik,S., Sahu,P.P., Srivastava,P.S. and Prasad,M. (2012) NAC proteins: regulation and role in stress tolerance. *Trends Plant Sci.*, **17**, 369–381.
28. Kim,H.S., Park,B.O., Yoo,J.H., Jung,M.S., Lee,S.M., Han,H.J., Kim,K.E., Kim,S.H., Lim,C.O., Yun,D.J. *et al.* (2007) Identification of a calmodulin-binding NAC protein as a transcriptional repressor in Arabidopsis. *J. Biol. Chem.*, **282**, 36292–36302.
29. Yamaguchi,M., Ohtani,M., Mitsuda,N., Kubo,M., Ohme-Takagi,M., Fukuda,H. and Demura,T. (2010) VND-INTERACTING2, a NAC domain transcription factor, negatively regulates xylem vessel formation in Arabidopsis. *Plant Cell*, **22**, 1249–1263.
30. Lee,M.G., Wynder,C., Cooch,N. and Shiekhattar,R. (2005) An essential role for CoREST in nucleosomal histone 3 lysine 4 demethylation. *Nature*, **437**, 432–435.
31. Zhang,C.J., Ning,Y.Q., Zhang,S.W., Chen,Q., Shao,C.R., Guo,Y.W., Zhou,J.X., Li,L., Chen,S. and He,X.J. (2012) IDN2 and its paralogs form a complex required for RNA-directed DNA methylation. *PLoS Genet.*, **8**, e1002693.
32. Trapnell,C., Pachter,L. and Salzberg,S.L. (2009) TopHat: discovering splice junctions with RNA-Seq. *Bioinformatics*, **25**, 1105–1111.
33. Zhang,X., Bernatavichute,Y.V., Cokus,S., Pellegrini,M. and Jacobsen,S.E. (2009) Genome-wide analysis of mono-, di- and trimethylation of histone H3 lysine 4 in Arabidopsis thaliana. *Genome Biol.*, **10**, R62.
34. Roudier,F., Ahmed,I., Berard,C., Sarazin,A., Mary-Huard,T., Cortijo,S., Bouyer,D., Caillieux,E., Duvernois-Berthet,E., Al-Shikhley,L. *et al.* (2011) Integrative epigenomic mapping defines four main chromatin states in Arabidopsis. *EMBO J.*, **30**, 1928–1938.
35. Langmead,B., Trapnell,C., Pop,M. and Salzberg,S.L. (2009) Ultrafast and memory-efficient alignment of short DNA sequences to the human genome. *Genome Biol.*, **10**, R25.
36. Zhang,Y., Liu,T., Meyer,C.A., Eeckhoute,J., Johnson,D.S., Bernstein,B.E., Nussbaum,C., Myers,R.M., Brown,M., Li,W. *et al.* (2008) Model-based Analysis of ChIP-Seq (MACS). *Genome Biol.*, **9**, R137.
37. Feng,Z., Zhang,B., Ding,W., Liu,X., Yang,D.L., Wei,P., Cao,F., Zhu,S., Zhang,F., Mao,Y. *et al.* (2013) Efficient genome editing in plants using a CRISPR/Cas system. *Cell Res.*, **23**, 1229–1232.
38. Schmid,M., Davison,T.S., Henz,S.R., Pape,U.J., Demar,M., Vingron,M., Scholkopf,B., Weigel,D. and Lohmann,J.U. (2005) A gene expression map of Arabidopsis thaliana development. *Nat. Genet.*, **37**, 501–506.
39. Hao,Y.-J., Song,Q.-X., Chen,H.-W., Zou,H.-F., Wei,W., Kang,X.-S., Ma,B., Zhang,W.-K., Zhang,J.-S. and Chen,S.-Y. (2010) Plant NAC-type transcription factor proteins contain a NARD domain for repression of transcriptional activation. *Planta*, **232**, 1033–1043.
40. Tran,L.S., Nakashima,K., Sakuma,Y., Simpson,S.D., Fujita,Y., Maruyama,K., Fujita,M., Seki,M., Shinozaki,K. and Yamaguchi-Shinozaki,K. (2004) Isolation and functional analysis of Arabidopsis stress-inducible NAC transcription factors that bind to a drought-responsive cis-element in the early responsive to dehydration stress 1 promoter. *Plant Cell*, **16**, 2481–2498.
41. Ogo,Y., Kobayashi,T., Nakanishi Itai,R., Nakanishi,H., Kakei,Y., Takahashi,M., Toki,S., Mori,S. and Nishizawa,N.K. (2008) A novel NAC transcription factor, IDEF2, that recognizes the iron deficiency-responsive element 2 regulates the genes involved in iron homeostasis in plants. *J. Biol. Chem.*, **283**, 13407–13417.
42. Zhong,R., Lee,C. and Ye,Z.H. (2010) Global analysis of direct targets of secondary wall NAC master switches in Arabidopsis. *Mol. Plant*, **3**, 1087–1103.
43. Braun,P., Carvunis,A., Charloteaux,B., Dreze,M., Ecker,J.R., Hill,D.E., Roth,F.P., Vidal,M., Galli,M., Balumuri,P. *et al.* (2011) Evidence for network evolution in an Arabidopsis interactome map. *Science*, **333**, 601–607.
44. Pien,S., Fleury,D., Mylne,J.S., Crevillen,P., Inze,D., Avramova,Z., Dean,C. and Grossniklaus,U. (2008) ARABIDOPSIS TRITHORAX1 dynamically regulates FLOWERING LOCUS C activation via histone 3 lysine 4 trimethylation. *Plant Cell*, **20**, 580–588.
45. Kim,S.Y., He,Y., Jacob,Y., Noh,Y.S., Michaels,S. and Amasino,R. (2005) Establishment of the vernalization-responsive, winter-annual habit in Arabidopsis requires a putative histone H3 methyl transferase. *Plant Cell*, **17**, 3301–3310.
46. Tamada,Y., Yun,J.Y., Woo,S.C. and Amasino,R.M. (2009) ARABIDOPSIS TRITHORAX-RELATED7 is required for methylation of lysine 4 of histone H3 and for transcriptional activation of FLOWERING LOCUS C. *Plant Cell*, **21**, 3257–3269.
47. He,Y., Michaels,S.D. and Amasino,R.M. (2003) Regulation of flowering time by histone acetylation in Arabidopsis. *Science*, **302**, 1751–1754.
48. Jiang,D., Yang,W., He,Y. and Amasino,R.M. (2007) Arabidopsis relatives of the human lysine-specific Demethylase1 repress the expression of FWA and FLOWERING LOCUS C and thus promote the floral transition. *Plant Cell*, **19**, 2975–2987.
49. Liu,F., Quesada,V., Crevillen,P., Baurle,I., Swiezewski,S. and Dean,C. (2007) The Arabidopsis RNA-binding protein FCA requires a lysine-specific demethylase 1 homolog to downregulate FLC. *Mol. Cell*, **28**, 398–407.
50. Chen,Q., Wang,Q., Xiong,L. and Lou,Z. (2011) A structural view of the conserved domain of rice stress-responsive NAC1. *Protein Cell*, **2**, 55–63.
51. Welner,D.H., Lindemose,S., Grossmann,J.G., Møllegaard,N.E., Olsen,A.N., Helgstrand,C., Skriver,K. and Lo Leggio,L. (2012) DNA binding by the plant-specific NAC transcription factors in crystal and solution: a firm link to WRKY and GCM transcription factors. *Biochem. J.*, **444**, 395–404.
52. Jensen,M.K., Kjaersgaard,T., Nielsen,M.M., Galberg,P., Petersen,K., O'Shea,C. and Skriver,K. (2010) TheArabidopsis thalianaNAC transcription factor family: structure–function relationships and determinants of ANAC019 stress signalling. *Biochem. J.*, **426**, 183–196.